

Article

Spatial Patterns and Associations of Tree Species in a Temperate Forest of National Forest Park, Huadian City, Jilin Province, Northeast China

Longhui Lin ^{1,†} , Xin Ren ^{1,†}, Hideyuki Shimizu ², Chenghuan Wang ^{1,*}  and Chunjing Zou ^{1,3,*}

¹ Shanghai Key Lab for Urban Ecological Processes and Eco-Restoration, School of Life Science, East China Normal University, Shanghai 200062, China; 51261300146@stu.ecnu.edu.cn (L.L.); 51151300201@stu.ecnu.edu.cn (X.R.)

² National Institute for Environmental Studies, 16-2 Onogawa, Tsukuba 305-8506, Ibaraki, Japan; hideshow@hotmai.com

³ College of Life Science & Technology, Xinjiang University, Urumqi 830017, China

* Correspondence: chwang@bio.ecnu.edu.cn (C.W.); cjzou@bio.ecnu.edu.cn (C.Z.)

† These authors contributed equally to this work.

Abstract: Analyzing the spatial patterns and associations among tree species may help to elucidate the importance of the ecological processes behind population formation and the mechanisms of species coexistence. To explore this mechanism, we mapped and studied eight dominant tree species in Korean pine broad-leaved mixed forests in a temperate forest region in Jilin Province, Northeast China. The spatial distribution patterns and spatial associations of the eight dominant tree species at different life history stages and spatial scales were analyzed using the second-order spatial point pattern method based on pair correlation functions. The results indicated the following: (1) The diameter class structure of all individuals in the plots showed an obvious “L” shape, indicating that the community was well regenerated and belonged to a growing stand. (2) The distribution of trees was affected by scale, size, and habitat heterogeneity. The degree of aggregation decreased as the diameter class increased. (3) Out of the 56 pairs of individuals, a small number showed a significant correlation, while most were negatively correlated. It is concluded that seed dispersal limitations, competitive ability, and topography and light requirements may influence the spatial distribution and association of species to maintain species coexistence and diversity in Korean pine broad-leaved mixed forests. The results can provide insights into the ecological processes of population assembly, the mechanisms of species coexistence, and the relationship between forest management and restoration.

Keywords: temperate forest; spatial pattern; spatial association; point pattern analysis; pair correlation function



Citation: Lin, L.; Ren, X.; Shimizu, H.; Wang, C.; Zou, C. Spatial Patterns and Associations of Tree Species in a Temperate Forest of National Forest Park, Huadian City, Jilin Province, Northeast China. *Forests* **2024**, *15*, 714. <https://doi.org/10.3390/f15040714>

Academic Editor: Russell G.

Congalton

Received: 18 March 2024

Revised: 10 April 2024

Accepted: 16 April 2024

Published: 18 April 2024



Copyright: © 2024 by the authors. Licensee MDPI, Basel, Switzerland. This article is an open access article distributed under the terms and conditions of the Creative Commons Attribution (CC BY) license (<https://creativecommons.org/licenses/by/4.0/>).

1. Introduction

Forests are among the most biodiverse and ecologically important ecosystems on Earth, providing essential ecosystem services and habitats for countless species [1]. Among them, temperate forests occupy a prominent position, characterized by their wide geographic distribution and diverse species composition [2]. These forests support complex communities of tree species, whose spatial patterns are indicative of the intricate ecological processes at work.

Spatial patterns of tree species are a crucial structural feature of communities and are the result of the interaction of various factors over many years within a biological community [3]. Understanding the spatial distribution of tree species is fundamental to unraveling the dynamics of forest ecosystems [4]. Spatial patterns reflect the outcomes of various ecological processes such as seed dispersal, competition, and environmental heterogeneity and provide insights into species coexistence, community dynamics, and

ecosystem functioning [5–7]. Additionally, studying changes in spatial patterns and species associations can inform the development of potential conservation strategies to maintain a baseline of species coexistence in natural communities [8].

Some researchers have studied the spatial patterns of species and have found that spatial patterns are highly dependent on scale [9–11]. While plant populations may follow an aggregated distribution at some scales, their distribution may be random or regular at other scales [12]. Previous studies have focused on small sample sizes, limiting the validity of their results. To determine the spatial distribution patterns of species, it is urgent to investigate the factors that influence them, as these patterns change depending on the scale of analysis. However, traditional spatial pattern analysis methods, such as the χ^2 test, ANOVA, and nearest neighbor distance analysis, are insufficient to answer the aforementioned questions [13]. Therefore, the method of second-order statistics was developed [14]. This method is based on the distance between a pair of points, allowing it to overcome the limitations of traditional methods that can only analyze spatial distribution patterns at a single scale [15]. Second-order statistics has therefore been applied to multiscale studies of the spatial distribution of species and their spatial associations [16].

Previous studies have examined the spatial distribution of species on a large scale and their relationship to biodiversity conservation [15,17–20]. These studies generally found a significant correlation between the diameter at breast height (DBH) and the age of individuals of the same species in the same living environment [21,22]. Therefore, population spatial patterns are commonly studied using size class (DBH class) rather than age class. In the last decade, research has increasingly focused on the study of spatial patterns and associations at different life stages or age classes [23,24]. Ecologists study spatial patterns at different stages of the life history or age to determine the underlying mechanisms of these processes and the scale at which they operate. Comparative studies of various successional species can reveal the relationships between their distribution and their specific habitat requirements [25]. However, studies on temperate forests often fail to consider the various successional species. Several recent studies have examined the spatial patterns among congeneric species. The researcher conducted a study to understand the mechanisms for the coexistence of several tree species in a one-square-kilometer patch of temperate forest by comparing distribution patterns of sympatric populations [26]. Some research investigated the spatial distribution and interrelationships of four species at different life stages in a 9-hectare plot of a temperate forest. The study revealed that the coexistence of these species may be influenced by seed dispersal limitation, landscape spatial structure, and the need for specific topography [27]. Analyzing the spatial distribution patterns and correlations among individuals at different life stages is helpful in understanding the spatial and temporal dynamics of a population [28].

The Korean pine broad-leaved mixed forest is the climax vegetation type of Northeast China and is widely distributed in the temperate forests of the region. The ecosystem in Northeast China is of paramount importance due to its large biomass, high biodiversity, and complex community structure [29–31]. Previous studies on the distribution of key species in these forests, especially on the northern slope of Changbai Mountain, have used various methods, including χ^2 tests, variance/mean ratio tests, mean square zone tests, and covariance analyses, with mixed results [32]. Recent studies have used methods such as point pattern analysis to simulate the spatial distribution of dominant tree species, revealing differences in spatial patterns of *Pinus koraiensis* among forest types and growth stages [33,34]. The China Forest Diversity Research Network (CFDRN) was established in 2004, and the Korean pine broadleaf woodland in Changbai Mountain is the earliest and largest forest in the network. The establishment of these forest plots further promotes the study of the spatial patterns of temperate broad-leaved Korean pine forests. For example, Zhang et al. investigated the spatial patterns and relationships between *P. koraiensis* and *Tilia amurensis* in different forest layers, revealing a mainly positive correlation and indicating *T. amurensis* as a beneficial companion species for *P. koraiensis* [32]. These studies, carried

out under different conditions and at different scales using different analyses, have led to different conclusions.

In this study, we compared the population structure, spatial distribution patterns, and spatial associations of eight co-occurring species with two different DBH classes in a 1.44 ha mixed broad-leaved Korean pine forest to gain insight into their coexistence and regeneration processes. We addressed the following questions: (1) Are there significant differences in population structure and spatial distribution patterns among these eight major species in the forest? (2) What are the effects of habitat heterogeneity on the spatial distribution patterns of juvenile and adult trees? (3) How do the spatial patterns and associations change with the scale and size class?

2. Methods

2.1. Study Site

The study site was located in the Hongshi National Forest Park in Huadian City, Jilin Province, Northeast China (42.82° N, 127.13° E) (Figure 1). The park covers an area of approximately 28,577 ha and is characterized by hilly mountainous terrain, with elevations ranging from 400 m to 1000 m. The study site is dominated by the north temperate continental monsoon climate with short, rainy summers and long, cold winters. The average annual air temperature is 3.4° C. The average annual precipitation is 700–800 mm, most of which falls during the short summer growing season from July to August. There are 125 frost-free days and the main soil types are dark brown, albic, alluvium, and meadow. The forest park has been spared from logging and other human disturbances for the last 30 years.

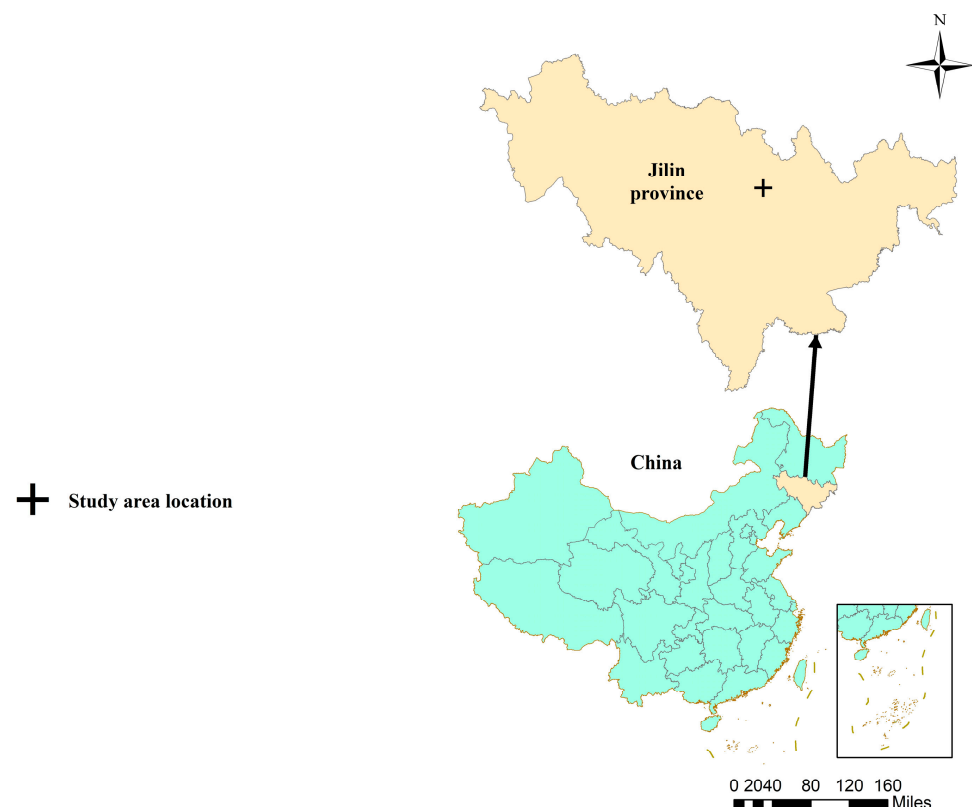


Figure 1. Map of study sites.

In addition to its ecological significance, Hongshi National Forest Park is also of socio-economic importance to the local community. The park has been spared from logging and other human disturbance in recent years, contributing to the preservation of biodiversity and ecosystem services. The park also serves as a recreational area for local residents and tourists, attracting visitors from nearby towns and providing opportunities for ecotourism

development. The conservation efforts and sustainable management practices implemented in the park are essential to maintaining the ecological integrity and promoting the socio-economic well-being of the region.

The main tree species include *P. koraiensis*, *Abies holophylla*, *Juglans mandshurica*, *Fraxinus mandchurica*, *Phellodendron amurense*, *Ulmus japonica*, *Quercus mongolica*, *T. amurensis*, *A. triflorum*, *A. mono*, and *A. pseudosieboldianum*.

2.2. Data Collection

A stem-mapped plot measuring 1.44 hectares (120 m × 120 m) was established in a mixed broadleaf Korean pine forest. This forest is the dominant vegetation type in the region in terms of species composition and stand structure. To enable systematic sampling, the plot was divided into 144 consecutive 10 m × 10 m quadrats. All trees within each sample plot were counted, and their species were identified and recorded in a data table along with their scientific names. The number of trees with a diameter at breast height (DBH) ≥ 3.1 cm was also recorded for each plot. Photographs of trees were taken for species that could not be identified in the field during the inventory. Subsequently, taxonomists and existing floras and taxonomic guides of Changbai Mountain were consulted to determine the species' names [35]. DBH was measured at 1.3 m above the ground using a diameter tape or calipers. The study recorded the geographic coordinates of each tree using a GPS device to obtain relative geographic coordinates, in addition to measuring DBH and identifying the species.

2.3. Data Analysis

In this paper, two life stages were designated for the tree species according to DBH: juvenile (DBH < 10 cm) and adult (DBH ≥ 10 cm) [36]. An exception was *Syringa reticulata*, which was classified according to different DBH measurements (juvenile for DBH < 4 cm and adult for DBH ≥ 4 cm) because it is a smaller sub-tree, understory species [37]. To achieve the required sample size, we only analyzed those species with more than 30 individuals in the population, which included eight species in the adult class, *S. reticulata*, *P. koraiensis*, *J. mandshurica*, *A. holophylla*, *A. pseudosieboldianum*, *A. triflorum*, *A. mono*, and *T. amurensis*, and five species in the juvenile class, *P. koraiensis*, *J. mandshurica*, *A. pseudosieboldianum*, *A. triflorum*, and *A. mono* (Figure 2).



Figure 2. Photographs of study species. Pictured from the first row onwards from left to right are *S. reticulata*, *P. koraiensis*, *J. mandshurica*, *A. holophylla*, *A. pseudosieboldianum*, *A. triflorum*, *A. mono*, and *T. amurensis*.

In recent years, several different two-order statistical methods have been used to analyze spatial point pattern analysis [38–42]. Among them, Ripley’s K-function has been widely used [38,43–45]. The calculation formula for the K-function is as follows:

$$K(r) = \frac{A}{n^2} \sum_{i=1}^n \sum_{j=1}^n \frac{I_r(d_{ij})}{W_{ij}} (i \neq j), \quad (1)$$

where A is the area of the sample plot, n is the total number of species in the sample plots, r is the radius of the circle, $I_r(d_{ij})$ is the indicator function, and d_{ij} is the distance between the center point i and point j . When $d_{ij} \leq r$, $I_r(d_{ij}) = 1$ and $d_{ij} > r$, $I_r(d_{ij}) = 0$, W_{ij} is the weight. However, when the K-function is used to analyze spatial patterns, a distance (scale) is included for all the information in the circle: as the distance (scale) increases, the results for the large distances (scales) include the information of the small distances (scales) [46,47]. This cumulative calculation confuses the effects of large and small scales [38,44].

We used Ripley’s K-function and the pair correlation function to examine the spatial patterns among the trees [48]. Point pattern analysis, a statistical principle, was first proposed by Ripley and has subsequently been continuously improved and developed since then. The details of these mathematical principles can be found in previous publications [38,48]. In this paper, using the coordinates of individual plants in space as the basic data, each individual was considered as a point in two-dimensional space so that all the individuals together formed a point map. The spatial patterns were analyzed according to the point map [49].

The pair correlation function $g(r)$ was derived from Ripley’s K-function [38]:

$$g(r) = \frac{1}{2\pi r} \frac{dK(r)}{d(r)}. \quad (2)$$

In this equation, the area of a circle with radius r is replaced by the area of a circle with a given radius, making it a probability density function, which is useful for exploring ecological pattern formation [47,49]. The pair correlation function includes univariate and bivariate analyses. The univariate statistics are used to analyze the spatial patterns of a single species, while the bivariate statistics are used to analyze the spatial associations of two species. For a univariate point pattern, $g(r) > 1$ indicates that the points are aggregated at a given distance, r , and $g(r) < 1$ indicates that they are regularly distributed, while $g(r) = 1$ indicates a random distribution. For a bivariate point pattern, $g_{12}(r) > 1$ indicates a positive association (attraction) between the two patterns at a given distance, r , while $g_{12}(r) < 1$ indicates a negative interaction (repulsion) between them at distance r , and $g_{12}(r) = 1$ indicates no interaction.

In our study, univariate statistics were used to test the spatial distributions of eight species (for the adult class) and five species (for the juvenile class) at different scales. The complete spatial random model (CSR) was used as the null model to test whether habitat heterogeneity affects the spatial distribution of juveniles and adult trees. At a small scale, aggregation may be caused by interactions between plants. At scales greater than 10 m, if the adult trees are aggregated, it can be inferred that habitat heterogeneity is at work [50]. In addition, we also used the heterogeneous Poisson process (HP) to examine the distribution patterns of dominant populations excluding habitat heterogeneity. Bivariate statistics were used to determine whether there was a spatial relationship between two different species or two different life stages (DBH classes). The null model was a heterogeneous Poisson process based on a nonparametric intensity estimation using the Epanechnikov kernel [51]. For adult trees, we left the locations of species 1 untouched and distributed the trees of species 2 using the heterogeneous Poisson process described above, and for adult trees and juveniles, we kept the locations of the adult trees constant and used the locations of the juveniles to calculate the simulated values.

To analyze the spatial patterns of the plant population with fine precision, we used a grid size of 1 m × 1 m and a ring width of 3 m. Significant departures from the null model

were assessed using the fifth lowest and fifth highest values of 199 Monte Carlo simulations of the null model to generate approximately 95% simulation envelopes. For all analyses, we performed the goodness-of-fit (GoF) test over the interval 0–20 m to assess departures from the null model. The results were retained for further analysis if the p value of the GoF test was less than 0.05. All analyses were performed using Programita software (November 2018 version), and all figures were generated in Sigmaplot 14.0 [47].

3. Results

3.1. Population Structure

We documented 1351 free-standing living individuals of 22 species belonging to 12 families and 14 genera. The stand was an old-growth forest with a reversed J-shaped distribution of tree diameters when pooled for all species. Of the individuals, 70.61% were in the 1–20 cm DBH class (Figure 3). As *S. reticulata* is a shrub, the majority of individuals of this species have a diameter at breast height (DBH) of less than 10 cm. *P. koraiensis* was present in all DBH classes, with more juveniles (DBH \leq 10 cm) and adult trees than trees with DBH \geq 40 cm. *T. amurensis* had an L-shaped distribution of diameters and relatively more adult trees. Six of the eight species had a similar L-shaped distribution with a high concentration of younger trees, indicating that the forest was regenerating.

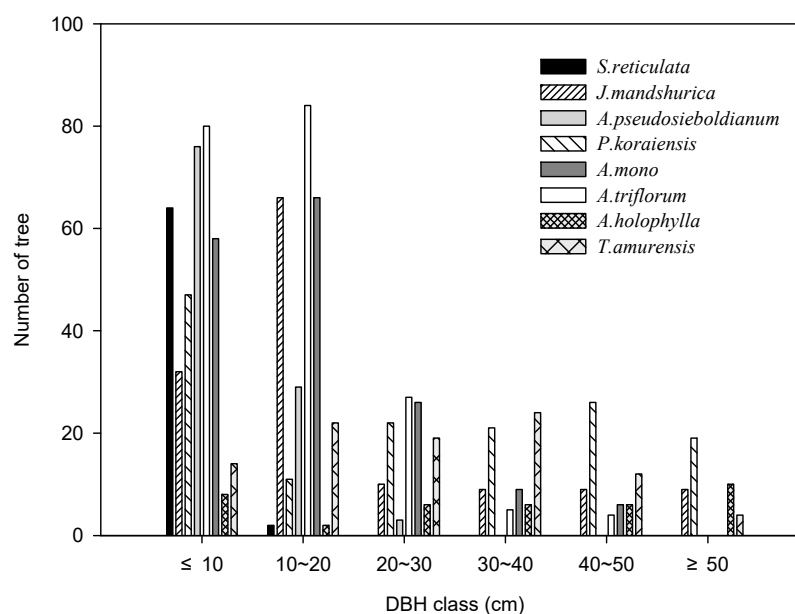


Figure 3. Diameter distribution for all live trees of each major species.

3.2. Spatial Patterns

All species showed aggregated distributions at a certain scale (Figure 4). The GoF test revealed a significant departure from the CSR null model for all eight species and for both DBH classes. The spatial analysis did not include *S. reticulata*, *A. holophylla*, or *T. amurensis* due to the small number of younger trees in the plot. Of the eight main species, five in the juvenile class and eight in the adult class exhibited an aggregated distribution at small scales. This aggregation decreased as the scale increased, resulting in a random distribution. The aggregated distribution was very obvious among these eight species, and the ranges of the aggregated distributions were as follows: *P. koraiensis* at 0–2 m and 8 m scales; *A. pseudosieboldianum* at 0–47 m and 49–59 m; *A. triflorum* at 0–4 m and 12–14 m; *A. mono* at 0–34 m, 39 m, and 44–46 m; *J. mandshurica* was mainly concentrated at 0–38 m; *S. reticulata* at 0–20 m and 24–27 m; *A. holophylla* at 0–1 m, 3–4 m, 10–13 m, and 36–38 m; and *T. amurensis* at 0–1 m, 3 m, 10–11 m, 18–21 m, 25–26 m, and 30–31 m. Among them, there were obvious clustered distributions from small scales to medium scales for *J. mandshurica*, *A. pseudosieboldianum*, and *A. mono*.

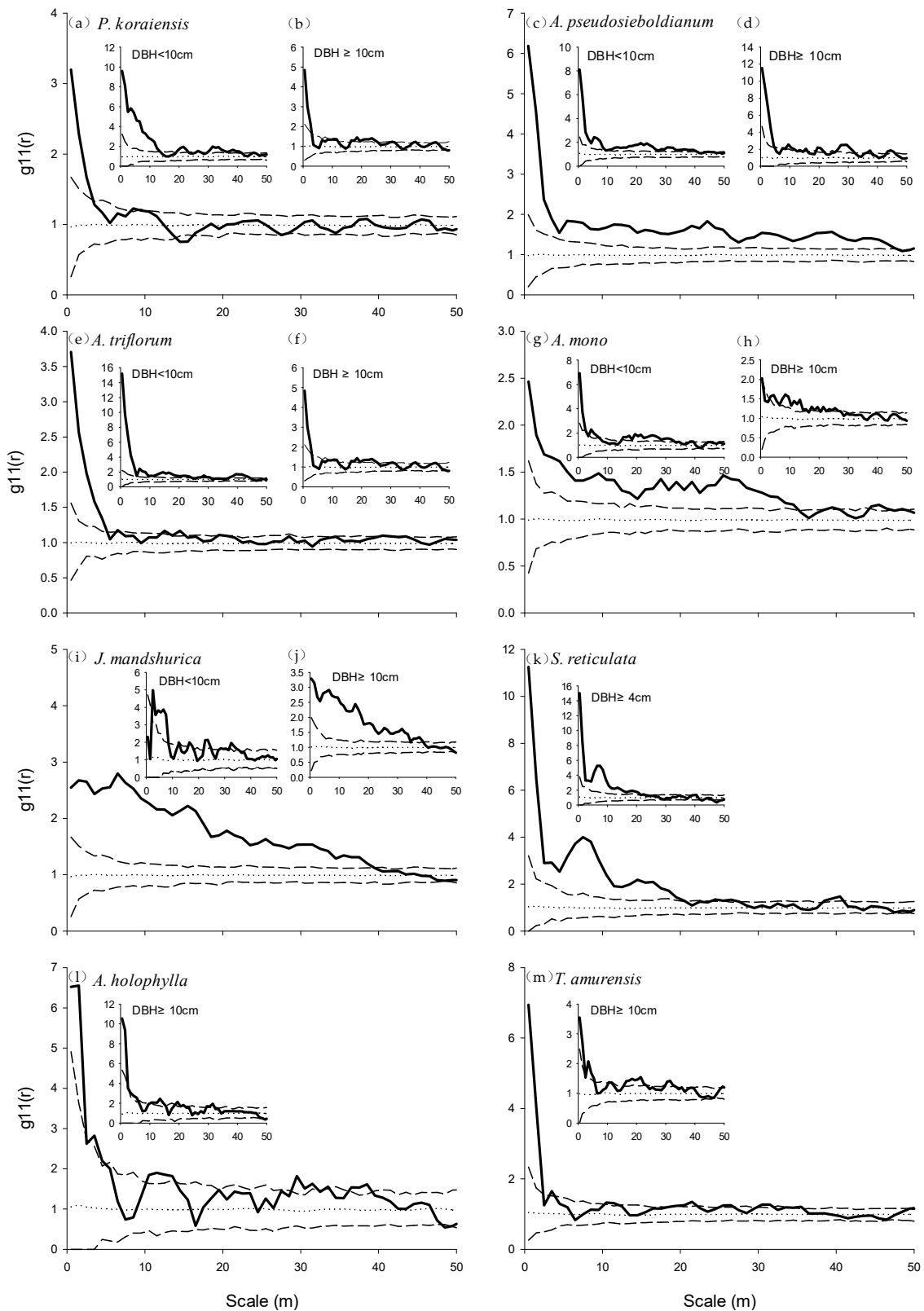


Figure 4. Univariate point pattern analyses of eight species under the CSR null model. The larger figures show the spatial distribution of all individuals of the 8 species, and the insets show the analyses of the two different size classes. Solid lines indicate the observed pair correlation functions; dotted lines indicate the expected g function under the CSR null model; and short-dashed lines indicate the simulation envelopes being the fifth-lowest and fifth-highest $g(r)$ values of the 199 Monte Carlo simulations of the null model. Points above the upper envelopes stand for aggregation, points between the envelopes stand for random, and points below the envelopes stand for regular.

P. koraiensis juveniles showed aggregated distributions at the scales of 0–13 m, 19–22 m, and 30–41 m, and the adult trees showed aggregation at scales of 0–2 m, 10–11 m, 16–25 m, 30–31 m, 38 m, and 44–45 m. *J. mandshurica* juveniles were found to be aggregated at scales of 2–7 m, 16–17 m, 23–24 m, 30–38 m, and 32–35 m, while the adult trees were aggregated at a scale of 0–38 m. At other scales, the distribution was random. The seedlings of *A. pseudosieboldianum* were also found to be aggregated at scales of 0–8 m, 10–40 m, and 44 m, while the adults showed an aggregated distribution at scales of 0–4 m, 7–13 m, 15 m, 19–21 m, 26–31 m, and 35–37 m. The juvenile trees of *A. triflorum* were clustered at scales of 0–23 m, 26–30 m, and 37–43 m, and the adult trees were found to be aggregated at scales of 1–3 m and 19 m. *A. mono* juvenile trees were in an aggregated distribution at scales of 0–1 m, 4–6 m, 15–32 m, and 38–39 m, while the adult trees aggregated at 3–15 m, 17–19 m, 21 m, and 23–27 m. For *P. koraiensis* and *Acer* spp., the degree of aggregation of juvenile trees at small scales was relatively high in comparison to the adult class: as DBH increased, the degree of aggregation significantly decreased. *S. reticulata* was found to be aggregated at scales of 0–20 m and 22 m. *A. holophylla* showed an aggregated distribution at scales of 3–5 m, 10–14 m, 19–21 m, and 29–31 m. *T. amurensis* aggregated at scales of 0–1 m, 3–5 m, 10 m, and 16–22 m. In conditions of habitat heterogeneity, *J. mandshurica* adult trees mainly aggregated at scales of 0–40 m, while aggregated distributions of both the adult trees and juveniles of the remaining species were mainly concentrated at the 0–20 m scale.

Figure 5 shows the spatial distributions of the eight main populations (five species for juvenile trees and eight species for adult trees) in the absence of habitat heterogeneity. The GoF test also revealed a significant departure from the HP null model for seven species: four species of adult trees and four species of juvenile trees. Obviously, compared with the distribution patterns of the juvenile trees, the scale range of aggregation significantly decreased for the adult trees, and there were more random distributions in the adult age class. The aggregated distributions of the eight populations were mainly concentrated at 0–5 m, and only *S. reticulata* and *J. mandshurica* clustered at 0–10 m scales. The aggregated distributions of the five species of juvenile trees were mainly concentrated at 0–10 m. For adult trees, only *S. reticulata* was aggregated at 0–10 m, with the adult class of the remaining seven species mainly aggregating at 0–5 m.

P. koraiensis juveniles exhibited an aggregated distribution in the range of 0–7 m and a random distribution at other scales. Adult trees were only found to aggregate within the range of 0–1 m. *J. mandshurica* juveniles showed an aggregated distribution at 2 m and 4–7 m, and the adult trees were clustered in the range of 0–5 m. Juvenile trees of *J. mandshurica* showed an aggregated distribution at scales of 0–2 m and 23 m and at 0–3 m for the adult trees. The juvenile trees of *A. triflorum* clustered at the 0–3 m and 39–43 m scales, but the adult trees showed a random distribution at all scales. At the 0–1 m scale, only the juveniles of *A. mono* were clustered, while the adult trees were randomly distributed at all scales. The degree of aggregation in the juvenile class species decreased significantly at small scales as DBH increased, except for *A. pseudosieboldianum*. Both *S. reticulata* and *A. holophylla* showed aggregated distributions in the range of 0–1 m, while *T. amurensis* was aggregated at all scales. In addition to adult *A. triflorum* trees, *A. mono* and *T. amurensis* were randomly distributed at all scales. The other species showed a similar spatial distribution being aggregated at small scales and gradually becoming less so as the scale increased, ultimately resulting in a random distribution. After habitat heterogeneity was excluded, the five tree species in the juvenile class tended to aggregate at the 0–10 m scale, and eight tree species in the adult class tended to aggregate at the 0–5 m scale, with the exception of *S. reticulata*, which mainly aggregated at the scale of 0–10 m.

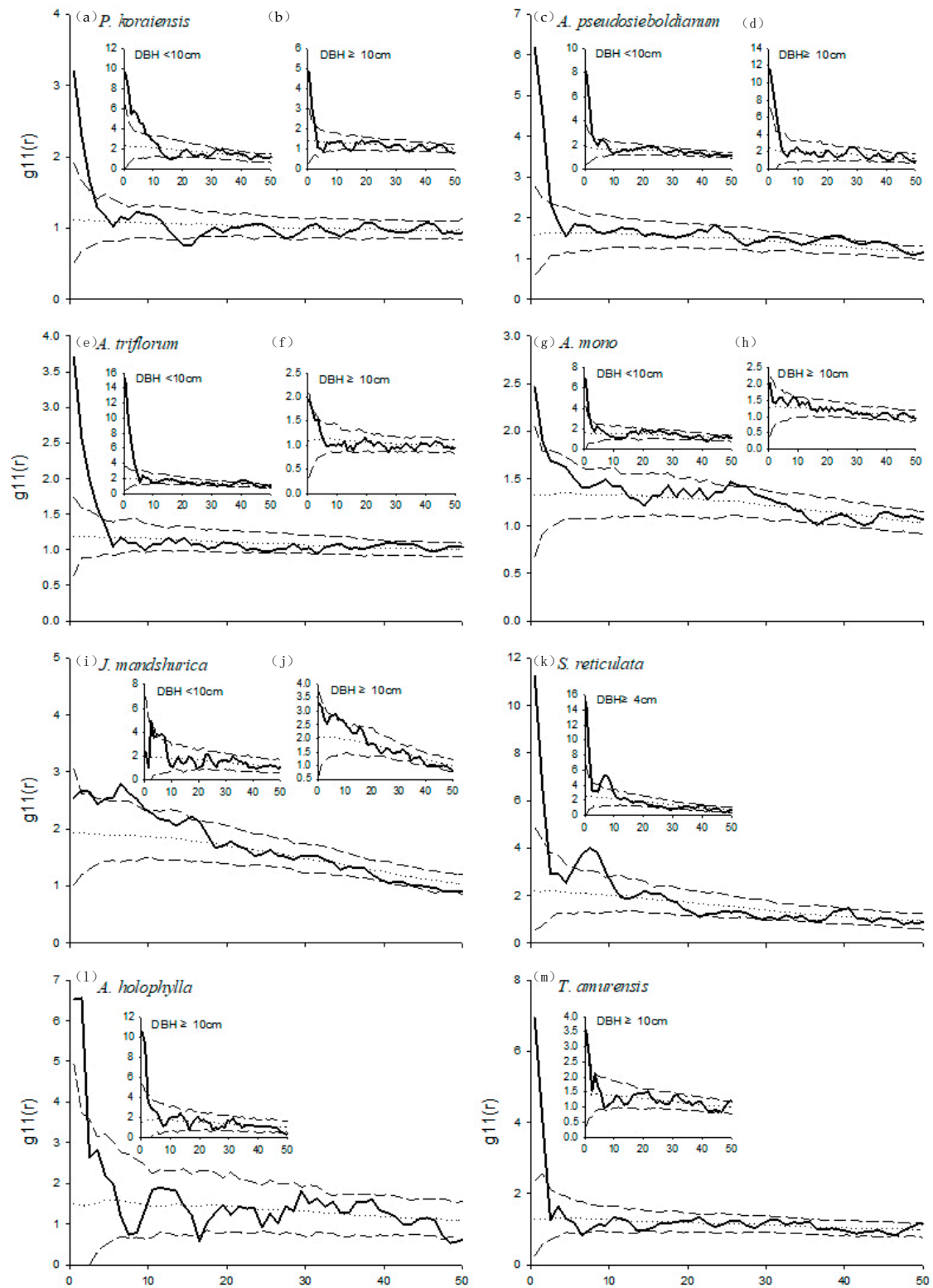


Figure 5. Univariate point pattern analyses of eight species under the HP null model. The larger figures show the spatial distribution of all individuals of the 8 species, and the insets show the analyses of the two different size classes. Solid lines indicate the observed pair correlation functions; dotted lines indicate the expected g function under the HP null model; and short-dashed lines indicate the simulation envelopes being the fifth-lowest and fifth-highest $g(r)$ values of the 199 Monte Carlo simulations of the null model. Points above the upper envelopes stand for aggregation, points between the envelopes stand for random, and points below the envelopes stand for regular.

Regardless of whether habitat heterogeneity is included or excluded, the population as a whole, including juveniles and adult trees, showed similar spatial patterns (Figures 4 and 5). Specifically, there was aggregation at small scales, which gradually decreased as the scale increased, and finally, there was random distribution at large scales. The results showed that the spatial distribution patterns of species varied with scale. Notably, when excluding habitat heterogeneity, all species aggregated at significantly reduced scales and mainly concentrated at 0–5 m or 0–10 m. This indicates that aggregation at small scales may be caused by the biological characteristics of the species, such as seed dispersal limitation. However, the large-scale aggregation suggests that habitat heterogeneity affects these species.

3.3. Spatial Associations

Using bivariate statistics, we performed a total of 56 (8×7), 56 (8×7), and 20 (5×4) bivariate point pattern analyses for all individuals of the eight species in the adult class and the five species in the juvenile class. The results of the GoF test showed significant negative associations (repulsion) for three pairs: *J. mandshurica* vs. *A. pseudosieboldianum* at 1–4 m, *A. pseudosieboldianum* vs. *A. triflorum* at 1–4 m, and *A. triflorum* vs. *A. pseudosieboldianum* at 0–4 m. Additionally, positive associations (attraction) were found for seven pairs at small scales (refer to Table 1). At scales of 0–4 m, *A. triflorum* and *A. pseudosieboldianum* showed a negative association. Six out of seven pairs with positive associations were found to be symmetric (in *S. reticulata* vs. *J. mandshurica*, *P. koraiensis* vs. *A. mono*, and *P. koraiensis* vs. *A. holophylla*). At scales of 0–2 m and 6–9 m, there was a positive association between *S. reticulata* and *J. mandshurica*, while at scales of 0–9 m, there was a positive association between *J. mandshurica* and *S. reticulata*. Additionally, at scales of 1–4 m, there was a significant positive association between *P. koraiensis* and *A. mono*. At scales of 1–3 m, there is a positive association between *P. koraiensis* and *A. holophylla*. Similarly, at scales of 2–5 m, there is a positive association between *A. holophylla* and *P. koraiensis*. Additionally, the pair of *P. koraiensis* and *A. pseudosieboldianum* showed a positive association at scales of 7–9 m. In our methodology, we described the pair correlation function $g(r)$, which represents the probability of a species occurring within a certain distance (scale) from a given point, forming a ring around it. The ranges mentioned in the text, such as 0–2 m and 6–9 m, denote the widths of these rings, which are incrementally increasing. Thus, any scale can be calculated accordingly. However, the data in the table are aggregated based on a 5 m scale, which includes all rings within that width. We also analyzed the spatial associations among the individuals of each species in two size classes. When comparing the spatial associations among small trees (DBH < 10 cm, or DBH < 4 cm for *S. reticulata*), the GoF test revealed that only 2 of 20 pairs significantly departed from the HP null model (Figure 6); *P. koraiensis* vs. *A. mono* and *A. mono* vs. *P. koraiensis*, which showed positive correlations at small scales of 2–3 m.

When comparing the spatial associations among large trees (DBH \geq 10 cm or DBH < 4 cm for *S. reticulata*), the GoF test detected significant departures from the HP null model for 15 species pairs (Figure 7). In 13 cases, the small-scale association was negative (repulsion), while in the other two cases, the small-scale association was positive (attraction). The two pairs of departing species were *S. reticulata* vs. *J. mandshurica* and *J. mandshurica* vs. *S. reticulata*, which showed positive correlations at scales of 0–2 m. The negative associations of the remaining 13 species appeared at different scales: *J. mandshurica* vs. *A. pseudosieboldianum* at 3–6 m scales, *P. koraiensis* vs. *A. pseudosieboldianum* at 1 m and 3–7 m scales, *P. koraiensis* vs. *A. triflorum* at 5–35 m scales, *P. koraiensis* vs. *A. mono* at 2–41 m scales, *P. koraiensis* vs. *S. reticulata* at 1–7 m and 20–24 m scales, *P. koraiensis* vs. *A. holophylla* at 5–41 m and 45–47 m scales, *P. koraiensis* vs. *T. amurensis* at 2–37 m and 41–46 m scales, *S. reticulata* vs. *P. koraiensis* at 1–25 m scales, *S. reticulata* vs. *A. pseudosieboldianum* at 2–11 m and 15–20 m scales, *S. reticulata* vs. *A. triflorum* at 0–33 m scales, *S. reticulata* vs. *A. mono* at 0–31 m scales, *S. reticulata* vs. *A. holophylla* at 1–38 m scales, and *S. reticulata* vs. *T. amurensis* at 0–32 m scales.

Table 1. Analyses of the spatial associations of eight species in the study plot.

Species 1	Species 2	p Values	Scales (m)							
			0–5	5–10	10–15	15–20	20–25	25–30	30–40	40–50
<i>S. reticulata</i>	<i>J. mandshurica</i>	0.0005	+(no)	+(no)	no	no	no(–)	no	no	no
<i>J. mandshurica</i>	<i>S. reticulata</i>	0.01	+	+	no	no	no	no	no	no(–)
<i>J. mandshurica</i>	<i>A. pseudosieboldianum</i>	0.035	–(no)	no(–)	no	no	no	no	no	no
<i>P. koraiensis</i>	<i>A. pseudosieboldianum</i>	0.02	no	+(no)	no	no(–)	no	no	no(+)	no
<i>P. koraiensis</i>	<i>A. mono</i>	0.005	+(no)	no	no(+)	no	no	no	no	no
<i>P. koraiensis</i>	<i>A. holophylla</i>	0.005	+(no)	no(+)	no	no	no	no	no	no
<i>A. mono</i>	<i>P. koraiensis</i>	0.015	+(no)	no						
<i>A. holophylla</i>	<i>P. koraiensis</i>	0.005	+(no)	no(+)	no	no	no	no	no	no
<i>A. triflorum</i>	<i>A. pseudosieboldianum</i>	0.005	–	no(–)	no	no	no	no	no	no
<i>A. pseudosieboldianum</i>	<i>A. triflorum</i>	0.02	–(no)	no						

Note: The bivariate statistic of the pair correlation function was used to analyze the spatial associations among eight species under the heterogeneous Poisson null model. “+” stands for a positive association, “no” stands for no spatial association, “–” stands for a negative association, “+(no)” indicates the positive association is greater than no spatial association, “no(+)” indicates that no spatial association is greater than the positive association, “–(no)” indicates the negative association is greater than no spatial association, and “no(–)” indicates that no spatial association is greater than a negative association at the studied scales. The p values were calculated based on the GoF test. Only species pairs with a p value < 0.05 are shown in the table.

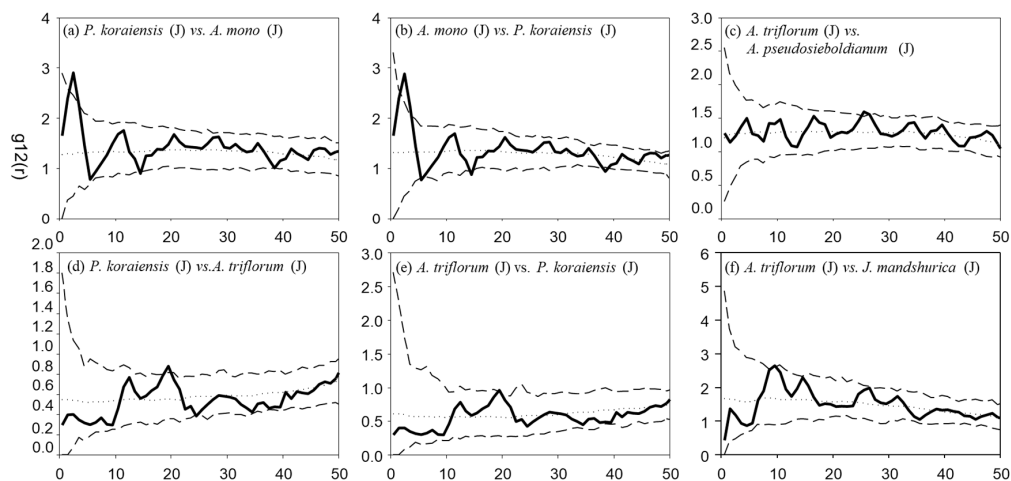


Figure 6. Examples of interspecies associations among juvenile species. Solid lines indicate ring statistics ($g_{12}^{(r)}$); dotted lines indicate the expected g function under the HP null model; and short-dashed lines indicate the simulation envelopes being the fifth-lowest and fifth-highest $g_{12}^{(r)}$ values of the 199 Monte Carlo simulations of the null model. Points above the upper envelopes stand for positive associations, points between the envelopes stand for independent patterns, and points below the envelopes stand for negative associations.

When comparing the spatial associations between large and juvenile trees of these species, the GoF test showed positive associations for 4 out of 40 species pairs and negative associations for only 2 out of 40 species pairs at small scales (Figure 8). At scales of 0–4 m, there was a negative correlation between *A. triflorum* and *J. mandshurica* and a negative association between *A. triflorum* and *A. pseudosieboldianum* at scales of 2–4 m. The four remaining species pairs showed positive correlations at different scales. Specifically, *S.*

reticulata vs. *A. triflorum* at 3 m and 6–11 m scales, *A. mono* vs. *P. koraiensis* at 1–4 m scales, *A. holophylla* vs. *P. koraiensis* at 2–6 m scales, and *T. amurensis* vs. *A. pseudosieboldianum* at 0–2 m scales. The other large trees did not show any association with the juvenile trees.

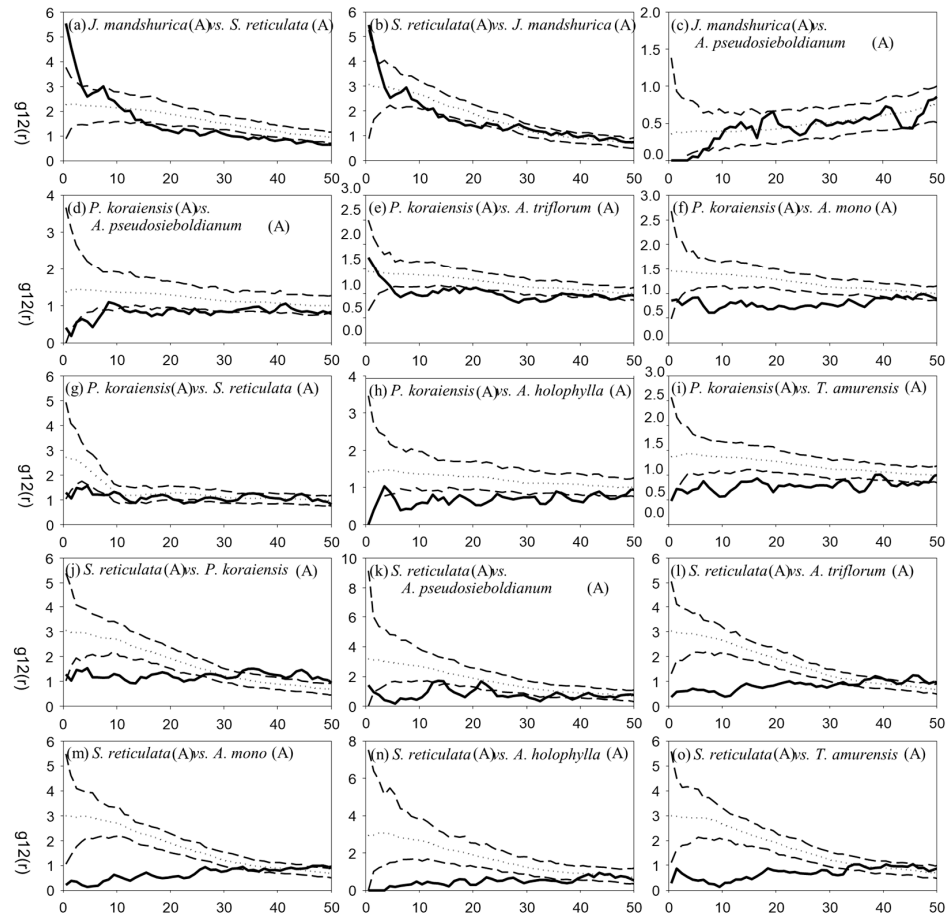


Figure 7. Examples of interspecies associations among adult species. All other symbols and descriptions are the same as in Figure 6.

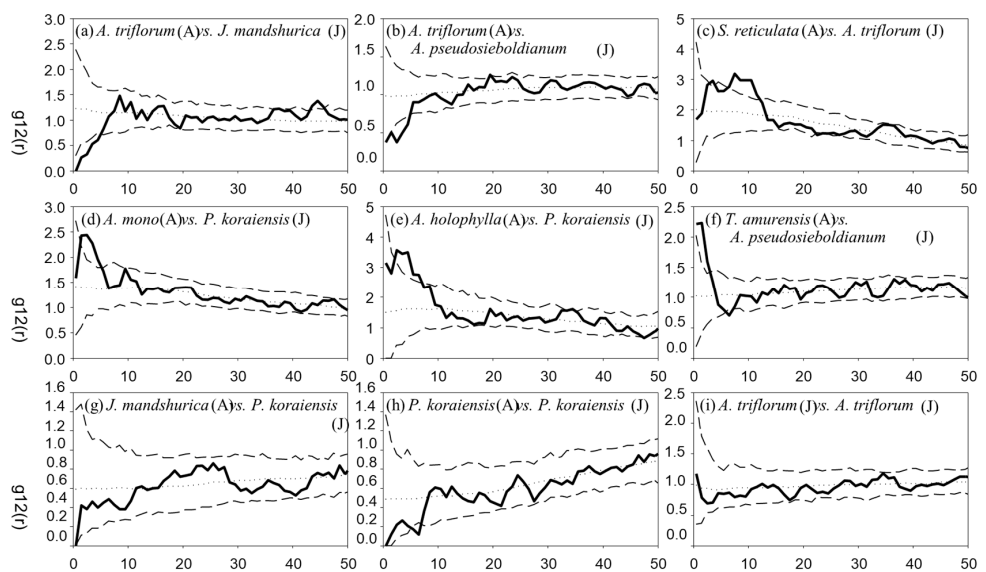


Figure 8. Examples of intra- and interspecies associations among juvenile species and adult species. All other symbols and descriptions are the same as in Figure 6.

4. Discussion

4.1. Spatial Distribution Patterns and Influencing Factors

Our study examined the spatial distribution and interspecific relationships of eight major tree species in a mixed broad-leaved Korean pine forest. The populations in the stand exhibited an aggregation pattern at small scales, transitioning to a more random distribution as the scale increased. This randomness at larger scales can be attributed to the abundance of Korean pine and the number of trees with larger diameter at breast height (DBH), which exacerbates competition for resources such as light and space, leading to a more stable community structure [22]. Research has shown that species with larger seeds, lower maximum heights, and lower frequency of distribution of adult individuals are more spatially and temporally restricted [52]. These restrictions on seed dispersal have an impact on intraspecific competition and competitiveness, which further affects the spatial distribution of species in the community and thus maintains the diversity of the community. Furthermore, it was discovered that the topography and light requirements significantly influenced the distribution of species [53].

The study analyzed the impact of habitat heterogeneity on species distributions and found that excluding it led to smaller aggregation sizes for all species. This result is in line with previous research, including Sierra de Guadarrama's (2016) study, which highlighted the effects of habitat heterogeneity on species distributions at various scales [54]. We emphasized the significant influence of environmental factors on the distribution of woody plants, highlighting the close relationship between plant growth and environmental conditions. To mitigate the effects of habitat heterogeneity on study results, we recommend controlling for variables, selecting appropriate study sites, and using multiple data analysis methods when investigating plant interactions.

Some sources suggest that closely related species with similar ecological features may not coexist. Interspecific competition is more likely to occur between such species, especially at small scales [55]. The GoF test revealed significant correlations between certain pairs of species. Notably, Korean pine was found to have significant associations with six other species, while it did not show any significant association with *J. mandshurica*. *S. reticulata* was significantly associated with all seven species. These associations were largely influenced by similarities in habitat requirements and dispersal limits, suggesting adequate resources for species coexistence [56]. However, the preponderance of negative correlations among adult species, particularly among those occupying different forest levels, suggests that interspecific competition is influenced by biological traits [57].

4.2. Methodological Limitations

This study employs spatial point pattern analysis methods, such as Ripley's K-function and pair correlation function, to investigate the spatial distribution patterns of tree species. However, it is important to note that these methods have limitations that require attention.

Specifically, the cumulative calculation of these methods may obscure the spatial distribution patterns at different scales [50]. As the scale of analysis increases, results at larger scales may obscure subtle changes at smaller scales. Therefore, it is important to carefully evaluate the results of the analysis at different scales and note any possible differences.

Additionally, we used a specific spatial resolution and ring width in our analysis. Different parameter settings can produce varying results. Choosing a larger spatial resolution may result in a loss of detail in the spatial pattern, which can fail to capture aggregation or dispersion on small scales. Conversely, selecting a smaller spatial resolution may increase the computational effort of the analysis and lead to overfitting of the data, resulting in unstable results. Regarding the ring width, it is important to consider the impact of parameter selection on our analysis of clustering and dispersion at different scales. To ensure robust and reliable results, it is best practice to perform parameter sensitivity analysis and try different parameter combinations.

This study utilized the complete spatial random (CSR) model and the heterogeneous Poisson process (HP) as the basic models for spatial distribution. The CSR model assumes that points or species in a given area are distributed randomly, without spatial correlation or aggregation [58]. This ignores, to a certain extent, the influence of environmental and biological factors on spatial distribution, such as soil type, vegetation structure, and biological interactions. The heterogeneous Poisson process, on the other hand, assumes spatial heterogeneity but may oversimplify the expression of this heterogeneity and ignore some subtle spatial differences [58].

In natural ecosystems, spatial distribution is influenced by various complex factors, including soil properties, topography, hydrological conditions, vegetation structure, and biological interactions [59]. These factors can cause diverse patterns of spatial distribution, such as aggregated, dispersed, or random patterns. Therefore, simple spatial models may not adequately capture these complex ecological processes and spatial structures. Therefore, it is important to carefully consider the limitations of these models when interpreting the study results. It should be noted that actual ecosystems may have more complexity and variability.

4.3. Implications for Conservation

The findings of this study hold significant importance for forest conservation and management. Firstly, the study uncovers the spatial distribution and interconnections of major tree species in forests, providing crucial information for ecosystem conservation. Understanding the spatial distribution patterns of tree species can aid in identifying key habitat types and ecological processes, which can guide the selection of sites for conservation and the development of management measures [8]. Aggregation of tree species was observed at different scales, indicating habitat preferences and interspecific interactions under specific environmental conditions. These findings provide guidance for the conservation and restoration of critical habitat types.

Additionally, the results are instructive for the management and sustainable use of forest resources. Understanding the interconnections between tree species is crucial for comprehending their functions and roles in the ecosystem. This knowledge can aid in optimizing forest resource management practices and promoting the health and stability of forest ecosystems [3]. The spatial associations of different tree species at different growth stages demonstrate the importance of their interactions on forest structure and successional processes.

These findings provide guidance for promoting the natural regeneration and successional processes of tree species, as well as supporting the provision of ecosystem services and the sustainable utilization of forest resources. A deeper understanding of the spatial distribution and interconnections of tree species can improve the assessment of ecosystem service functions such as water conservation, soil retention, and carbon storage. This provides a basis for developing strategies to sustainably utilize and manage forest resources [4].

In summary, our findings are significant for guiding forest conservation and management practices, as well as improving the management and conservation of forest resources. By gaining an in-depth understanding of the spatial distribution and interconnections of tree species, forest ecosystems can be better protected and managed for healthy and sustainable ecosystem development.

5. Conclusions

The aim of this study was to investigate the spatial distribution and spatial associations of Korean pine broad-leaved mixed forests in Hongshi National Forest Park, Huadian City, Jilin Province. Based on the analysis of population structure, spatial distribution, and spatial associations, we suggest that differences among them are due to seed dispersal limitation, habitat heterogeneity, and tree species' demand for topography and light. In conclusion, this study presents the similarities and differences in population structure, spatial distribution patterns, and spatial associations among the eight main tree species

at various scales of the forest community. The results indicate that the spatial distribution pattern of these species becomes more random with increasing scale. Therefore, protecting the diversity and integrity of forest habitats is critical to maintaining tree species diversity and community stability. While forest gap dynamics, topography, and life history strategies may contribute to explaining species distributions, there is currently insufficient evidence to support the interpretation of species coexistence. Further studies are necessary to reveal the mechanisms behind species coexistence. Furthermore, additional research into the connections between species and other ecological factors such as temperature, humidity, soil conditions, and disturbance history may offer valuable insights into the mechanisms or reasons behind species coexistence.

Author Contributions: Investigation, X.R. and C.Z.; data curation, X.R.; writing—original draft, L.L. and X.R.; writing—review and editing, L.L., X.R., H.S., C.W. and C.Z.; project administration, C.Z.; funding acquisition, C.Z. All authors have read and agreed to the published version of the manuscript.

Funding: This research was funded by the National Natural Science Foundation of China grant number (No. 31100317, 31870405) and the Global Environmental Research Fund of the Ministry of the Environment of Japan.

Data Availability Statement: The data sets generated during and/or analyzed during the current study are available from the corresponding author upon request.

Acknowledgments: The authors thank all those who provided helpful suggestions and critical comments on this manuscript and anonymous reviewers. We thank Ma Huaiyu and Yu Lei for their field and experimental work. We also thank T. Wiegand for use of the Programita software.

Conflicts of Interest: The authors declare no conflicts of interest.

References

1. Raj, A.; Jhariya, M.K.; Banerjee, A.; Lal, B.; Mehergui, T.; Devi, A. Ghanshyam Forest for Sustainable Development. In *Land and Environmental Management through Forestry*; Wiley: Hoboken, NJ, USA, 2023; pp. 293–311.
2. Dreiss, L.M.; Volin, J.C. Forests: Temperate evergreen and deciduous. In *Terrestrial Ecosystems and Biodiversity*; CRC Press: Boca Raton, FL, USA, 2020; pp. 213–226.
3. Palaghianu, C.; Coşofreţ, C. Patterns of Forest Species Association in a Broadleaf Forest in Romania. *Forests* **2023**, *14*, 1118. [[CrossRef](#)]
4. Zhang, M.; Wang, J.; Kang, X. Spatial distribution pattern of dominant tree species in different disturbance plots in the Changbai Mountain. *Sci. Rep.* **2022**, *12*, 14161. [[CrossRef](#)]
5. Perea, A.J.; Wiegand, T.; Garrido, J.L.; Rey, P.J.; Alcántara, J.M. Spatial phylogenetic and phenotypic patterns reveal ontogenetic shifts in ecological processes of plant community assembly. *Oikos* **2022**, *2022*, e09260. [[CrossRef](#)]
6. Watt, A.S. Pattern and process in the plant community. *J. Ecol.* **1947**, *35*, 1–22. [[CrossRef](#)]
7. Gratzer, G.; Waagepetersen, R.P. Seed Dispersal, Microsites or Competition—What Drives Gap Regeneration in an Old-Growth Forest? An Application of Spatial Point Process Modelling. *Forests* **2018**, *9*, 230. [[CrossRef](#)]
8. Pang, S.E.; Ferry Slik, J.W.; Zurell, D.; Webb, E.L. The clustering of spatially associated species unravels patterns in Bornean tree species distributions. *bioRxiv*, **2022**. [[CrossRef](#)]
9. Xu, C.; Zhao, S.; Liu, S. Spatial scaling of multiple landscape features in the conterminous United States. *Landsc. Ecol.* **2020**, *35*, 223–247. [[CrossRef](#)]
10. Jin, L.S.; Yin, D.; Fortin, M.J.; Cadotte, M.W. The mechanisms generating community phylogenetic patterns change with spatial scale. *Oecologia* **2020**, *193*, 655–664. [[CrossRef](#)] [[PubMed](#)]
11. Zhou, Q.; Shi, H.; Shu, X.; Xie, F.; Zhang, K.; Zhang, Q.; Dang, H. Spatial distribution and interspecific associations in a deciduous broad-leaved forest in north-central China. *J. Veg. Sci.* **2019**, *30*, 1153–1163. [[CrossRef](#)]
12. Holmes, M.A.; Matlack, G.R. Spatial structure develops early in forest herb populations, controlled by dispersal and life cycle. *Oecologia* **2019**, *189*, 951–970. [[CrossRef](#)]
13. Ta, F.; Liu, X.D.; Liu, R.H.; Zhao, W.J.; Jing, W.M.; Ma, J.; Wu, X.R.; Zhao, J.-Z.; Ma, X. Spatial distribution patterns and association of *Picea crassifolia* population in Dayekou Basin of Qilian Mountains, northwestern China. *Chin. J. Plant Ecol.* **2020**, *44*, 1172. [[CrossRef](#)]
14. Deng, C.; Guan, Y.; Waagepetersen, R.P.; Zhang, J. Second-order quasi-likelihood for spatial point processes. *Biometrics* **2017**, *73*, 1311–1320. [[CrossRef](#)] [[PubMed](#)]
15. Ben-Said, M. Spatial point-pattern analysis as a powerful tool in identifying pattern-process relationships in plant ecology: An updated review. *Ecol. Process.* **2021**, *10*, 56. [[CrossRef](#)]

16. Ma, Z.B.; Xiao, W.F.; Huang, Q.L.; Zhuang, C.Y. A review of point pattern analysis in ecology and its application in China. *Acta Ecol. Sin.* **2017**, *37*, 6624–6632.
17. Condit, R. Research in large, long-term tropical forest plots. *Trends Ecol. Evol.* **1995**, *10*, 18–22. [[CrossRef](#)]
18. Harms, K.E.; Wright, S.J.; Calderón, O.; Hernandez, A.; Herre, E.A. Pervasive density-dependent recruitment enhances seedling diversity in a tropical forest. *Nature* **2000**, *404*, 493–495. [[CrossRef](#)]
19. Hubbell, S. *The Unified Neutral Theory of Biodiversity and Biogeography*; Princeton University Press: Princeton, NJ, USA, 2001; p. 32.
20. McMillan, N.A.; Fuhlendorf, S.D.; Davis, C.A.; Hamilton, R.G.; Neumann, L.K.; Cady, S.M. A plea for scale, and why it matters for invasive species management, biodiversity and conservation. *J. Appl. Ecol.* **2023**, *60*, 1468–1480. [[CrossRef](#)]
21. Keyimu, M.; Halik, U.; Betz, F.; Wumaier, G.; Dilimulati, G. Spatial-temporal change of DBH of *Populus euphratica* under artificial water conveyances. *J. For. Environ.* **2016**, *36*, 148.
22. Yang, H.B.; Guo, Q.X. Influence of topography and competitive factors on the relationship between DBH and age of Korean pine. *Acta Ecol. Sin.* **2016**, *36*, 6487–6495.
23. Liu, J.; Bai, X.; Yin, Y.; Wang, W.; Li, Z.; Ma, P. Spatial patterns and associations of tree species at different developmental stages in a montane secondary temperate forest of northeastern China. *PeerJ* **2021**, *9*, e11517. [[CrossRef](#)]
24. Peralta, A.L.; Escudero, A.; de la Cruz, M.; Sánchez, A.M.; Luzuriaga, A.L. Functional traits explain both seedling and adult plant spatial patterns in gypsum annual species. *Funct. Ecol.* **2023**, *37*, 1170–1180. [[CrossRef](#)]
25. Ulrich, W.; Zaplata, M.K.; Winter, S.; Fischer, A. Spatial distribution of functional traits indicates small scale habitat filtering during early plant succession. *Perspect. Plant Ecol. Evol. Syst.* **2017**, *28*, 58–66. [[CrossRef](#)]
26. Watanabe, S.; Maesako, Y. Co-occurrence pattern of congeneric tree species provides conflicting evidence for competition relatedness hypothesis. *PeerJ* **2021**, *9*, e12150. [[CrossRef](#)] [[PubMed](#)]
27. D’Andrea, R.; O’Dwyer, J.P. Competition for space in a structured landscape: The effect of seed limitation on coexistence under a tolerance-fecundity trade-off. *J. Ecol.* **2021**, *109*, 1886–1897. [[CrossRef](#)]
28. Traoré, A.S.; Kouassi, K.I.; Koné, M.; Gignoux, J.; Barot, S. Spatial patterns of a savanna palm tree *Borassus aethiopum* and its temporal variability. *J. Plant Ecol.* **2022**, *15*, 1049–1064. [[CrossRef](#)]
29. Wang, C.; Jiang, Q.O.; Deng, X.; Lv, K.; Zhang, Z. Spatio-temporal evolution, future trend and phenology regularity of net primary productivity of forests in Northeast China. *Remote Sens.* **2020**, *12*, 3670. [[CrossRef](#)]
30. Gu, Y.; Zhang, J.; Ma, W.; Feng, Y.; Yang, L.; Li, Z.; Guo, Y.; Shi, G.; Han, S. Ecological Factors Driving Tree Diversity across Spatial Scales in Temperate Forests, Northeast China. *Forests* **2023**, *14*, 1241. [[CrossRef](#)]
31. Liao, Z.; Su, K.; Jiang, X.; Zhou, X.; Yu, Z.; Chen, Z.; Wei, C.; Zhang, Y.; Wang, L. Ecosystem and Driving Force Evaluation of Northeast Forest Belt. *Land* **2022**, *11*, 1306. [[CrossRef](#)]
32. Zhang, J.; Hao, Z.Q.; Song, B.; Ye, J.; Li, B.H.; Yao, X.L. Spatial distribution patterns and associations of *Pinus koraiensis* and *Tilia amurensis* in broad-leaved Korean pine mixed forest in Changbai Mountains. *Chin. J. Appl. Ecol.* **2007**, *18*, 1681–1687.
33. Omelko, A.; Ukhvatkina, O.; Zhmerenetsky, A.; Sibirina, L.; Petrenko, T.; Bobrovsky, M. From young to adult trees: How spatial patterns of plants with different life strategies change during age development in an old-growth Korean pine-broadleaved forest. *For. Ecol. Manag.* **2018**, *411*, 46–66. [[CrossRef](#)]
34. Zhang, X.P.; Yu, L.Z.; Yang, X.Y.; Huang, J.Q.; Yin, Y. Population structure and dynamics of *Pinus koraiensis* seedlings regenerated from seeds in a montane region of eastern Liaoning Province, China. *Ying Yong Sheng Tai Xue Bao = J. Appl. Ecol.* **2022**, *33*, 289–296.
35. You, Z.; Wencai, W. *Flora of Changbai Mountain, China*; China Forestry Publishing House: Beijing, China, 2010.
36. Bradford, M.; Murphy, H.T. The importance of large-diameter trees in the wet tropical rainforests of Australia. *PLoS ONE* **2019**, *14*, e0208377. [[CrossRef](#)] [[PubMed](#)]
37. Xu, X.; Su, Z.; Yan, X. Effects of aspect on distribution pattern of *Taxus chinensis* population in Yele, Sichuan Province: An analysis based on patches information. *Ying Yong Sheng Tai Xue Bao = J. Appl. Ecol.* **2005**, *16*, 985–990.
38. Ripley, B.D. *Spatial Statistics*; Wiley & Sons: New York, NY, USA, 1981.
39. Gómez-Rubio, V. Spatial point patterns: Methodology and applications with R. *J. Stat. Softw.* **2016**, *75*, 1–6. [[CrossRef](#)]
40. Baddeley, A.; Rubak, E.; Turner, R. *Spatial Point Patterns: Methodology and Applications with R*; CRC Press: Boca Raton, FL, USA, 2015.
41. Xiang, Q.; Guo, Q.-j.; Ai, X.-r.; Yao, L.; Zhu, J.; Xue, W.-x.; Zhou, Y.; Zhao, H.-d.; Wu, J.-y. Variations on Stand Spatial Structure and Species Diversity in Different Spatial Scales. *For. Res.* **2022**, *35*, 151–160.
42. Liu, Q.; Wu, Z.W.; Lin, S.T.; Li, S.; Fang, Z.B. Spatial point pattern analysis of pine wilt disease occurrence and its influence factors. *Ying Yong Sheng Tai Xue Bao = J. Appl. Ecol.* **2022**, *33*, 2530–2538.
43. Self, S.; Overby, A.; Zgodic, A.; White, D.; McLain, A.; Dyckman, C. A Generalization of Ripley’s K Function for the Detection of Spatial Clustering in Areal Data. *arXiv* **2022**, arXiv:2204.10852.
44. Hohl, A.; Zheng, M.; Tang, W.; Delmelle, E.; Casas, I. Spatiotemporal point pattern analysis using Ripley’s K function. In *Geospatial Data Science Techniques and Applications*; CRC Press: Boca Raton, FL, USA, 2017; pp. 155–176.
45. Yates, L.A.; Brook, B.W.; Buettel, J.C. Spatial pattern analysis of line-segment data in ecology. *Ecology* **2022**, *103*, e03597. [[CrossRef](#)]
46. Condit, R.; Ashton, P.S.; Baker, P.; Bunyavejchewin, S.; Gunatilleke, S.; Gunatilleke, N.; Hubbell, S.P.; Foster, R.B.; Itoh, A.; LaFrankie, J.V.; et al. Spatial Patterns in the Distribution of Tropical Tree Species. *Science* **2000**, *288*, 1414–1418. [[CrossRef](#)]
47. Wiegand, T.A.; Moloney, K. Rings, circles, and null-models for point pattern analysis in ecology. *Oikos* **2004**, *104*, 209–229. [[CrossRef](#)]

48. Villegas, P.; Cavagna, A.; Cencini, M.; Fort, H.; Grigera, T.S. Joint assessment of density correlations and fluctuations for analysing spatial tree patterns. *R. Soc. Open Sci.* **2021**, *8*, 202200. [[CrossRef](#)]
49. Qu, H.; Zhang, Q. A method to improve Ripley's function to analyze spatial pattern by factor analysis. In Proceedings of the International Conference on Electronic Information Engineering and Data Processing (EIEDP 2023), SPIE, Nanchang, China, 17–19 March 2023; Volume 12700, pp. 562–566.
50. Wang, X.T.; Wang, D.J.; Li, H.B.; Tai, Y.; Jiang, C.; Liu, F.; Li, S.Y.; Miao, B.L. Cumulative effects of K-function in the research of point patterns. *Ying Yong Sheng Tai Xue Bao = J. Appl. Ecol.* **2022**, *33*, 1275–1282.
51. Wiegand, T.; Gunatilleke, S.; Gunatilleke, N. Species associations in a heterogeneous Sri Lankan dipterocarp forest. *Am. Nat.* **2007**, *170*, E77–E95. [[CrossRef](#)] [[PubMed](#)]
52. Zimback, L.B. Quais características influenciam a limitação de dispersão de sementes em uma comunidade arbórea tropical? Master's Thesis, Universidade de São Paulo, São Paulo, Brazil, 2017.
53. Gharti, P.; Dani, R.S.; Baniya, C.B. Relationship of topography and soil chemistry with plant richness and distribution in the temperate forest of Chandragiri hill, Kathmandu, Nepal. *Res. Sq.* **2023**. [[CrossRef](#)]
54. Lara-Romero, C.; de la Cruz, M.; Escribano-Ávila, G.; García-Fernández, A.; Iriondo, J.M. What causes conspecific plant aggregation? Disentangling the role of dispersal, habitat heterogeneity and plant–plant interactions. *Oikos* **2016**, *125*, 1304–1313. [[CrossRef](#)]
55. Anacker, B.L.; Strauss, S.Y. Ecological similarity is related to phylogenetic distance between species in a cross-niche field trans-plant experiment. *Ecology* **2016**, *97*, 1807–1818. [[CrossRef](#)] [[PubMed](#)]
56. Eigentler, L. Species coexistence in resource-limited patterned ecosystems is facilitated by the interplay of spatial self-organisation and intraspecific competition. *Oikos* **2021**, *130*, 609–623. [[CrossRef](#)]
57. Keddy, P.A. Competition. In *Causal Factors for Wetland Management and Restoration: A Concise Guide*; Keddy, P.A., Ed.; Springer International Publishing: Cham, Switzerland, 2023; pp. 73–80.
58. Qi, Y.; Zhang, G.; Xiong, Z.; Yang, T. Spatial point pattern analysis for coarse woody debris in karst mixed evergreen and deciduous broadleaved forest. *Acta Ecol. Sin.* **2019**, *39*, 4933–4943.
59. Gizachew, G. Spatial-temporal and factors influencing the distribution of biodiversity: A review. *ASEAN J. Sci. Eng.* **2022**, *2*, 273–284. [[CrossRef](#)]

Disclaimer/Publisher's Note: The statements, opinions and data contained in all publications are solely those of the individual author(s) and contributor(s) and not of MDPI and/or the editor(s). MDPI and/or the editor(s) disclaim responsibility for any injury to people or property resulting from any ideas, methods, instructions or products referred to in the content.